Eurasian Journal of Physics and Functional Materials

2019, 3(1), 31-39

Nucleon transfer in reactions ^{3}He+^{194}Pt, ^{45}Sc within time-dependent approach

V.V. Samarin[1,2,*], Yu.E. Penionzhkevich[1,3], M.A. Naumenko[1], N.K. Skobelev[1]

[1]Joint Institute for Nuclear Research, Russia

[2]Dubna State University, Russia

[3]National Research Nuclear University Mephi, Russia

[*]E-mail: samarin@jinr.ru

DOI: **10.29317/ejpfm.2019030104**
Received: 11.03.2019 - after revision

Theoretical description of the experimental data on the formation of various isotopes in reactions (^{3}He+^{194}Pt) and (^{3}He+^{45}Sc) requires taking into account neutron and proton transfer channels, as well as fusion-evaporation channels. To calculate the probabilities of nucleon transfer as well as transfer cross sections the time-dependent Schrodinger equation (TDSE) has been solved numerically. Fusion-evaporation was taken into account using the statistical model code of the NRV web knowledge base. Results of calculations are in agreement with experimental data.

Keywords: neutron and proton transfer, fusion-evaporation, time-dependent Schrodinger equation.

Introduction

The processes of neutron and proton transfer have been extensively studied both experimentally and theoretically. The theoretical description of experimental data on formation of gold isotopes in the (^{3}He+^{194}Pt)- reaction [1] and the ^{45}Ti isotope in the (^{3}He+^{45}Sc)- reaction [2] requires taking into account proton transfer channels. Considering these channels in the DWBA approximation provides (for the appropriate choice of parameters) satisfactory description of the experimental

angular distributions for energies much higher than the Coulomb barrier [3]. For near-barrier energies, however, oscillations in angular distributions are weakly pronounced, complicating determination of the optical potential parameters. It is easier in this case to compare theoretical calculations and experimental data on the formation cross sections of the reaction products.

The cross section for the ^{194}Au isotope formation in the (^{3}He+ ^{194}Pt)- reaction was measured by means of activation in [1]. Possible mechanisms of the ^{194}Au isotope formation include proton capture by the target nucleus with the loss of a neutron due to its evaporation (after the excitation associated with proton capture), or to its capture by the projectile nucleus (with the transformation of ^{3}He into ^{3}H). Another possible mechanism of ^{194}Au isotope formation, fusion of nuclei with evaporation of two neutrons and a proton, is of low probability because of the high Coulomb barrier for protons. For the (^{3}He+ ^{45}Sc)- reaction [2], the probability of ^{45}Ti isotope formation in the fusion-evaporation channel is much higher because of the lower Coulomb barrier.

In this work, fusion-evaporation was considered using the numerical code of the NRV web knowledge base [4, 5]. The numerical solution of the time-dependent Schrodinger equation taking into account spin-orbit interaction [6] was successfully used to calculate the cross sections of neutron transfer [7] and proton transfer [8] in reactions with the participation of ^{3}He nuclei. In this work, the time-dependent quantum approach is used to describe proton stripping from the ^{3}He nuclei in collisions with the ^{194}Pt and ^{45}Sc nuclei combined with neutron pickup from the target nuclei.

Theory

In [6-8], the time-dependent Schrodinger equation for protons or neutrons

$$ih\frac{\partial}{\partial t}\psi(\overset{r}{r},t)=\left\{-\frac{h^2}{2m}\Delta+W(\overset{r}{r},t)+\hat{V}_{LS}\ (\overset{r}{r},t)\right\}\psi(\overset{r}{r},t), \tag{1}$$

in combination with the classical equations of motion for nuclear centers of mass

$$m_1\ddot{\vec{r}}_1=-\nabla_{\vec{r}_1}V_{12}(\left|\vec{r}_1-\vec{r}_2\right|), m_2\ddot{\vec{r}}_2=-\nabla_{\vec{r}_2}V_{12}(\left|\vec{r}_2-\vec{r}_1\right|) \tag{2}$$

was used to describe transfer channels in collisions of atomic nuclei. Here, $\overset{I}{r}_1\ (t)$, $\overset{I}{r}_2\ (t)$ are the centers of nuclei with masses m_1, m_2 and V_{12}(r) is the potential energy of interaction of these nuclei, m is a proton (neutron) mass, ψ is a spinor wave function. Before touching of the surfaces of nuclei, the potential energy $W(\overset{I}{r},t)$ of the proton (neutron) and the operator $\widehat{V}_{LS}(\overset{I}{r},t)$ of spin-orbit interaction took the form of the sum of the central potentials V_i(r) and the operators $\widehat{V}_{LS.i}(\overset{I}{r},t)$ for a ^{3}He projectile nucleus (i=1) and for a heavy target nucleus (i=2). Residual interaction and pairing forces are not taken into account in our approach.

The initial condition for the proton wave function of the ^{3}He projectile nucleus was defined taking into account the long-range character of the Coulomb interaction

with the target nucleus. The proton wave function in an isolated projectile nucleus at a finite distance from the target nucleus was preliminarily subjected to slow (adiabatic) switching of the Coulomb interaction with the target nucleus. Thus, the effects of the proton cloud polarization were taken into account in the initial condition.

Results for (^{3}He+ ^{194}Pt) reaction

The initial condition for the proton wave function of the ^{3}He projectile nucleus was based on the shell model with the mean field potential $V_1(r)$ of the ^{3}He nucleus given in [7]. It differs from the Woods–Saxon potential by the maximum at zero providing better agreement with the experimental charge distribution [4]. The proton and neutron energy levels ε of the ^{3}He nucleus are shown in Figures 1(a) and 1(d), respectively. The Woods–Saxon form $V_2(r)$ was used as the nuclear part of the potential of proton (neutron) interaction with the heavy target nucleus. The values of the parameters were chosen from the condition of equality of the theoretical and experimental values of the energy E_8 of proton or neutron separation from the target [8].

After proton transfer to the ^{194}Pt nucleus, the $^{195}_{79}Au_{116}$ nucleus is formed. The upper single-particle proton levels of the ^{195}Au nucleus are shown in Figure 1(b). The neutron levels of the ^{194}Pt nucleus near the uppermost occupied level (Fermi level) are shown in Figure 1(e).

The typical pattern of the change in the proton probability density upon its stripping in the ^{3}He+ ^{194}Pt collision is shown in Figure 2. Here and below, the effective radius of the ^{3}He nucleus is $\bar{R}_1$ =2.2 fm, which is somewhat larger than its root-mean-square charge radius $R_{1ch} \approx 2$ fm [4], and the effective radius of the ^{194}Pt nucleus was determined according to the usual formula $\bar{R}_2 = 1.25A_2^{1/3} \approx 7.2$ fm.

For near-barrier energies [Figure 2a and Figure 2c], the structure of the probability density in the target nucleus corresponds to the dominant stripping of the neutron to the state with close energy $3_{s1/2}$ [see Figure 1(b)] of the produced ^{195}Au nucleus. Under the conditions of the slow relative motion of the colliding nuclei and the fast motion of the transferred proton, we observe an adiabatic regime [9] of probability density redistribution with the population of two-center states. In this case, only the high-lying states $2f_{7/2}$ and $1h_{9/2}$ can be populated, along with the state $3_{s1/2}$. The population of such states is higher in the grazing collisions at above-barrier energies [Figures 2(d)–2(f)], as can be seen from the increased probability density extending beyond the boundaries of the nucleus. As nuclei fly away and the distance between them grows, excitation can be reduced by the emission of both protons and neutrons. This gives the first mechanism of ^{194}Au isotope formation. The probability can be estimated using the formula

$$p_1 = C(p_0 - p^{(-)}), \tag{3}$$

where $C \leq 1$ is a variable (adjustable) parameter, p_0 is the probability for the proton

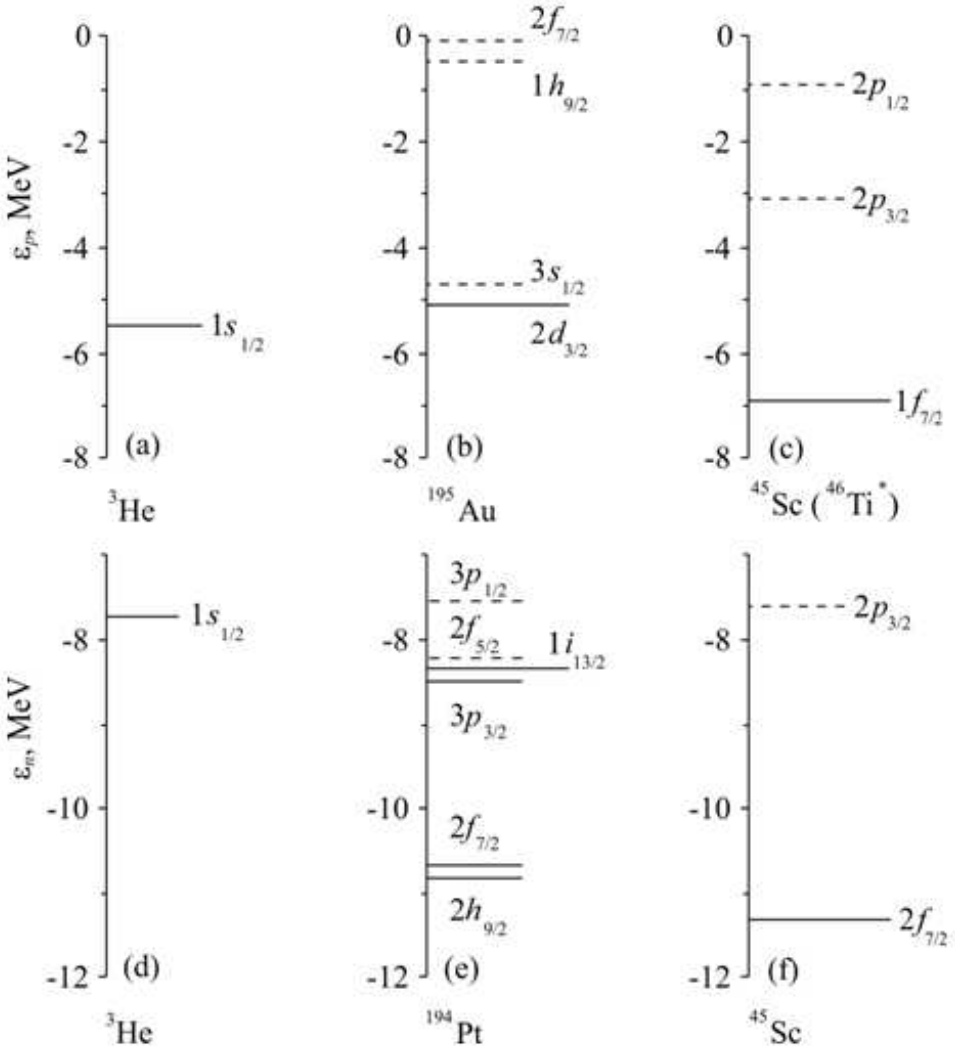

Figure 1. Proton energy levels in the shell model of ^{3} He (a), ^{195} Au (b), and $^{46}Ti^{*}$ (c) nuclei. Neutron energy levels in the shell model of ^{3} He (d), ^{194} Pt (e), and ^{45} Sc (f) nuclei. The longest and the dashed segments represent the uppermost occupied levels (Fermi levels) and the unoccupied levels, respectively.

from the ^{3} He nucleus to enter the region of the ^{194} Pt nucleus (not farther than the approximate radius of nuclear forces $R_{NN} \approx 3$ fm from its surface) in the time the projectile nucleus passes the target nucleus; and $p^{(-)}$ is the sum of populations of the initially free levels with energy $\varepsilon < 0$ in the ^{195} Au nucleus:

$$p^{(-)} = \lim_{t\to\infty} \sum_{k} \left|a_k(t)\right|^2, \tag{4}$$

where a_k are the coefficients of expansion of the time-dependent proton wave function (Figure 2) into the wave functions of the unoccupied single-particle states of the target nucleus. The difference $p_0 - p^{(-)}$ is the probability of occupation of the quasistationary states with energy $\varepsilon > 0$ in the potential well of the target nucleus surrounded by the Coulomb barrier with the lifetimes exceeding the interaction time of the nuclei. The residual interaction between the proton in these states and a neutron of the target nucleus may lead to the transition of this proton to unoccupied levels of the target nucleus accompanied by energy transfer to the neutron exceeding its separation energy.

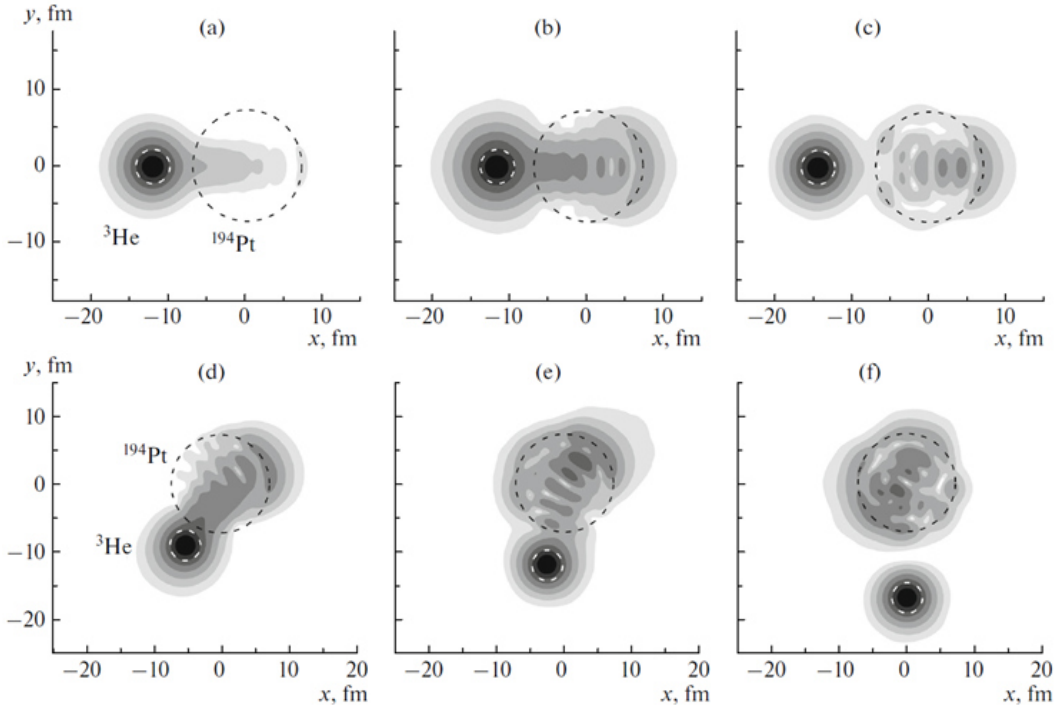

Figure 2. Evolution of the probability density for protons of the ^{3} He projectile nucleus in the collisions with the ^{194} Pt target nucleus for different values of center-of-mass energy E and impact parameter b : (a)–(c) E =19 MeV, b =0; (d)–(f) E =25 MeV, b =4.6 fm. The radii of the circles are equal to the effective radii of the nuclei. The time goes from left to right: (a)–(b)–(c), (d)–(e)–(f).

The second mechanism of ^{194} Au nucleus formation is a combination of neutron transfer from the ^{194} Pt nucleus to the ^{3} He nucleus and proton transfer in the opposite direction. The probability of this process is the product of the probability $p^{(-)}$ for proton stripping to the unoccupied single-particle states of the target nucleus and the probability $p_0^{'}$ for the neutron to enter the region of the projectile nucleus [7]

$$p_2 = p_0^{'} p^{(-)}, \tag{5}$$

During the transformation of the ^{3} He nucleus into ^{3} H, the mean field of the shell model can be assumed to vary slightly. The close energies of the neutron level in the projectile nucleus and the upper neutron levels of the ^{194} Pt nucleus [see Figure 1d and Figure 1e] in this case increases the probability of transfer between them. The most probable is neutron pickup from level $3p_{3/2}$ due to lower centrifugal barrier. Although the probability of neutron pickup from the broad potential well of the target nucleus to the narrow well of the projectile nucleus is low, the large number of neutrons (16) on the levels near the Fermi level increases the probability of pickup of one of them, and thus makes the contribution of the second mechanism of ^{194} Au formation noticeable.

The probabilities of the above processes are shown in Figure 3a as functions of minimum distance $R_{min}(b, E)$ between the centers of the colliding nuclei, where b is the collision impact parameter, and E is the center-of-mass energy. The probability logarithms can be smoothed by linear dependence

$$lgp_i(b, E) \approx A_i(E) - B_i(E) R_{min}(b, E), \tag{6}$$

with parameters A and B depending weakly on energy. The cross section of proton transfer (or a combination of proton and neutron transfer) was calculated by integrating the corresponding probability over the impact parameters of grazing collisions $b > b_{min}$:

$$\sigma(E) = \int_{b_{min}}^{\infty} p(b,E) b db, \tag{7}$$

The results of calculating the cross section of ^{194}Au isotope formation via proton stripping with neutron evaporation from the target nucleus and via proton stripping with neutron pickup are shown in Figure 3b along with the negligible contribution of the fusion-evaporation mechanism.

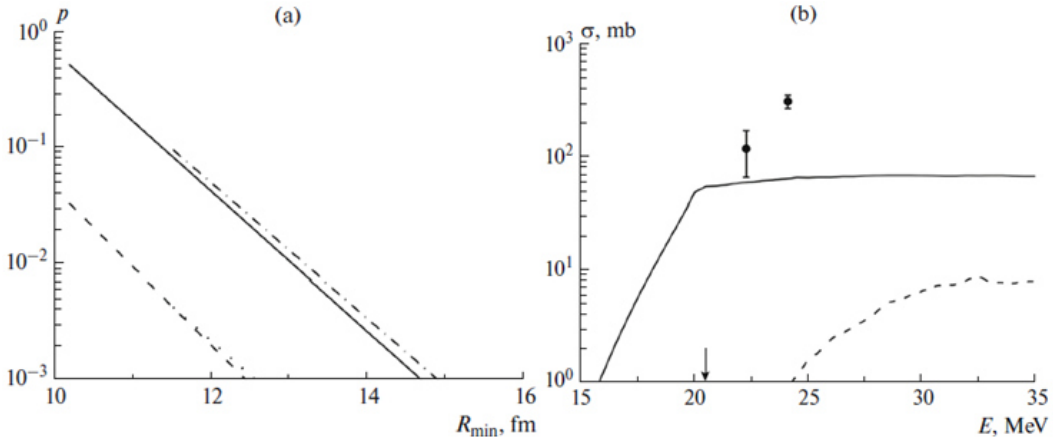

Figure 3. (a) Probability p_0 of proton transfer from the ^{3}He nucleus to the ^{194}Pt nucleus as a function of minimum distance R_{min} between the centers of the nuclei for center-of-mass energies E =25 MeV (solid line) and E =19 MeV(dash-dotted line) along with the probability $p^{(-)}$ of transfer to the discrete spectrum states with energies above the Fermi level for E =25 MeV (dashed line) and E =19 MeV (dotted line). (b) Cross section of ^{194}Au isotope formation in the ^{3}He+ ^{194}Pt reaction. Dots are experimental data from [1]. The solid line shows the contribution of neutron evaporation after proton transfer according to formula (3) with C=1; the dashed line shows the contribution of the fusion-evaporation channel calculated using the code of the NRV web knowledge base [4]. The arrow shows the position of the Coulomb barrier.

Results for (^{3}He+ ^{45}Sc) reaction

The nucleus $^{45}_{21}$Sc$_{24}$ has an unpaired proton on shell 1$f_{7/2}$. The experimental angular distributions for inelastic scattering given in [3] show that after proton transfer, the ground state of the $^{46}_{22}$Ti$_{24}$ nucleus with zero spin and two paired outer protons (on shell 1$f_{7/2}$) is produced with rather low probability. Therefore, the Ti nucleus is formed in exited states, $^{46}_{22}$Ti$^*_{24}$, with unpaired outer protons. In calculations, we used upper single-particle proton levels of the $^{46}_{22}$Ti$^*_{24}$ nucleus which were similar to the levels of the $^{45}_{21}$Sc$_{24}$ nucleus; they are shown in Figure 1(c). A typical pattern of the change in the proton probability density upon its stripping in the collision (^{3}He+ ^{45}Sc) nuclei is shown in Figure 4.

An adiabatic scenario [9] of probability density redistribution with population of two-center states is observed for near-barrier energies [Figure 4a and Figure 4c]. We can see that the structure of the probability density in the target nucleus corresponds to the dominant proton stripping to states 2$p_{3/2}$, 2$p_{1/2}$ of the formed ^{46}Ti nucleus

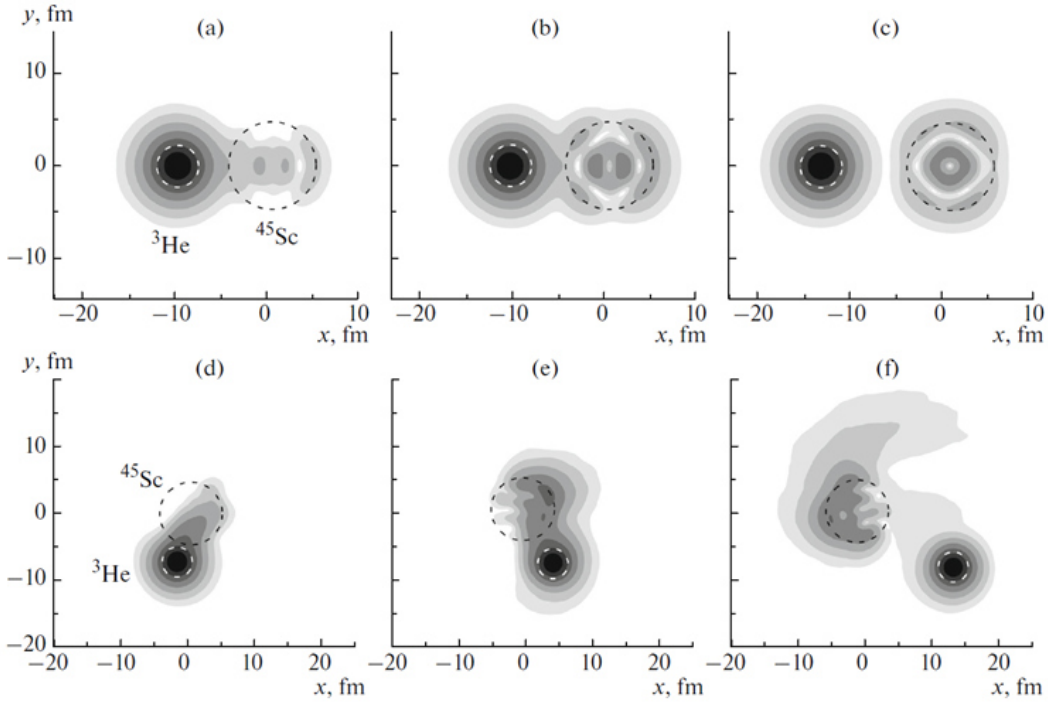

Figure 4. (a) Evolution of the probability density for protons of the ^{3} He projectile nucleus in the collisions with the ^{45} Sc target nucleus for different values of center-of-mass energy E and impact parameter b : (a)–(c) E =6 MeV, b =0; (d)–(f) E =35 MeV, b =7 fm. The radii of the circles are equal to the effective radii of the nuclei. The time goes from left to right: (a)–(b)–(c), (d)–(e)–(f).

because the angular dependence of the probability density corresponds to the Legendre polynomial $P_1(cos\theta) = \cos\theta$ and the radial dependence has one extra node in addition to the node at the center of the target nucleus (at r=0). Similar behavior was observed in [7] for neutron stripping from the state $1_{s1/2}$ of the ^{3} He nucleus to the state $2p_{3/2}$ of the Sc nucleus. Since the energies of these levels [see Figure 1d and Figure 1f] are close, the probability of neutron transfer is high. The probability of proton transfer is much lower because of the larger difference between the energies of the initial and final levels [see Figures 1a and Figure 1c]. The probability of neutron pickup by the ^{3} He nucleus from the lower levels of the ^{45} Sc nucleus in combination with proton stripping is extremely low for the same reason. In the case of grazing collisions with above-barrier energies [Figure 4d and Figure 4f], the rate of proton probability density redistribution is comparable to the relative velocity of the nuclei. This results in a nonadiabatic proton transfer regime [9] with the formation of highly excited states. As nuclei go away from each other, excitation can be reduced by the emission of both protons and neutrons. The probabilities of these processes are shown in Figure 5a as functions of the minimum distance between the centers of the colliding nuclei. The results of calculating the cross section of ^{45} Ti isotope formation via proton stripping with neutron evaporation from the target nucleus and via proton stripping with neutron pickup are shown in Figure 5b along with the contribution from the fusion-evaporation mechanism which is the main mechanism in this case.

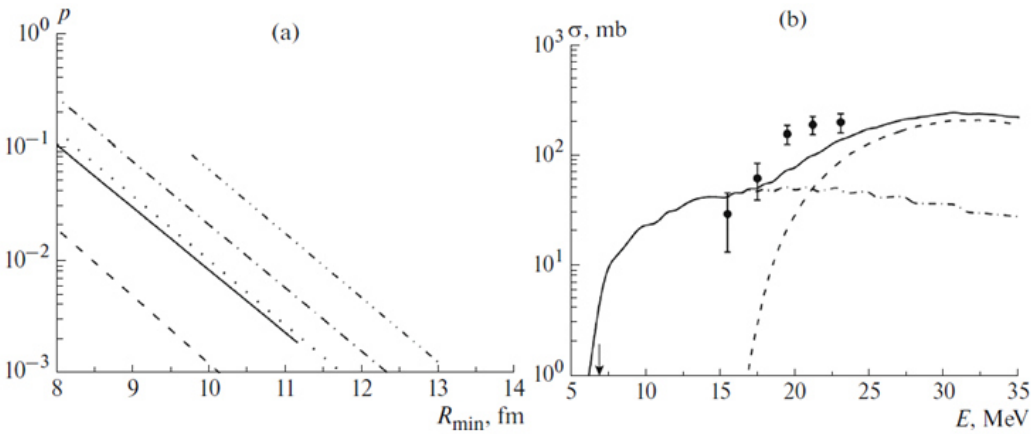

Figure 5. (a) Probability of proton transfer from the ^{3} He nucleus to the ^{45} Sc nucleus as a function of the minimum distance R_{min} between the centers of nuclei for center-of-mass energies E =35 MeV (solid line), E =16 MeV (dash-dotted line), and E =6 MeV (dashed-dot-dotted line), along with the probability $p^{(-)}$ of transfer to the discrete spectrum states with energies above the Fermi level: E =35 MeV (dashed line), E =16 MeV (dotted line), and E =6 MeV (coincides with the dashed-dot-dotted line). (b) Cross section of ^{45} Ti isotope formation in the (^{3} He+ ^{45} Sc) reaction. Dots are the experimental data from [1]. The dash-dotted line shows the estimated contribution of the neutron evaporation channel after proton transfer according to formula (3) with C=0.5; the dashed line shows the contribution of the fusion-evaporation channel calculated using the code of the NRV web knowledge base [4]; the solid line shows the sum of contributions of both channels. The arrow shows the position of the Coulomb barrier.

Discussion

Study of proton and neutron transfer can provide information on the properties of nuclear states of predominantly single-particle nature. For instance, the sufficiently large values of the transfer cross section at near-barrier energies indicate that the initial and final energy levels of the transferred nucleon are close (e.g., for the ^{3} He+ ^{194} Pt reaction). Vice versa, the low values of the transfer cross section at near-barrier energies indicate large difference between the initial and final energy levels of the transferred nucleon (e.g. for the ^{3} He+ ^{45} Sc reaction).

Conclusions

The experimental difference in the near-barrier energy dependence of formation cross sections for the ^{194} Au isotope in the (^{3} He+ ^{194} Pt) reaction and the ^{45} Ti isotope in the (^{3} He+ ^{45} Sc) reaction was explained by the difference in the proton and neutron shells of the target nuclei determining different character of evolution of the probability density for the proton of the projectile nucleus and the neutron of the target nucleus during the collision. Experimental data on the formation cross sections for a number of isotopes can be used for validation and refinement of theoretical models of nucleon transfer, nuclear fusion, and pre-equilibrium processes. The time-dependent approach used in this work can also be applied to calculation of the proton transfer cross sections in reactions with nuclei having proton halos (e.g. ^{8} B) and the cross sections of charged cluster (deuterons, α -clusters) transfer.

Acknowledgments

This work was supported by the Russian Science Foundation, Grant No. 17-12-01170.

References

[1] N.K. Skobelev et al., Phys. Part. Nucl. Lett. **11** (2014) 114.
[2] N.K. Skobelev et al., Bull. Russ. Acad. Sci.: Phys. **77** (2013) 795.
[3] R.W. Barnard, G.D. Jones, Nucl. Phys. A **111** (1968) 17.
[4] V.I. Zagrebaev et al., http://nrv.jinr.ru/nrv.
[5] A.V. Karpov et al., Nucl. Instrum. Methods Phys. Res. Sect. A **859** (2017) 112.
[6] V.V. Samarin, Phys. Atom. Nucl. **78** (2015) 128.
[7] M.A. Naumenko et al., Bull. Russ. Acad. Sci.: Phys. **80** (2016) 264.
[8] V.V. Samarin et al., Bull. Russ. Acad. Sci.: Phys. **82** (2018) 637.
[9] Yu.E. Penionzhkevich et al., Phys. Atom. Nucl. **80** (2017) 928.